eNeuro

Research Article: New Research | Disorders of the Nervous System

Altered Glycolysis and Mitochondrial Respiration in a Zebrafish Model of Dravet Syndrome

Metabolism in scn1Lab mutant Zebrafish

Maneesh G. Kumar[1], Shane Rowley[1], Ruth Fulton[1], Matthew T. Dinday[2], Scott C. Baraban[2] and Manisha Patel[1]

[1]*Department of Pharmaceutical Sciences, University of Colorado Anschutz Medical Campus, Aurora, CO 80045*
[2]*Department of Neurological Surgery, University of California San Francisco, San Francisco, CA 94143*

DOI: 10.1523/ENEURO.0008-16.2016

Received: 12 January 2016

Revised: 23 March 2016

Accepted: 24 March 2016

Published: 29 March 2016

Author contributions: M.G.K., S.C.B., and M.P. designed research; M.G.K. performed research; M.G.K. analyzed data; M.G.K., S.C.B., and M.P. wrote the paper; S.R., R.F., M.T.D., and S.C.B. contributed unpublished reagents/analytic tools.

Funding: DH | National Institute for Health Research (NIHR): 501100000272; R01NS39587(MP). DH | National Institute for Health Research (NIHR): 501100000272; R01NS079214(SCB).

Conflict of Interest: Authors report no conflict of interest.

Corresponding author: Manisha Patel, PhD, University of Colorado, Skaggs School of Pharmacy and Pharmaceutical Sciences, Mail Stop C238 V20-3119, 12850 E. Montview Blvd., Aurora, CO 80045. manisha.patel@ucdenver.edu

Cite as: eNeuro 2016; 10.1523/ENEURO.0008-16.2016

eNeuro

http://eneuro.msubmit.net

eN-NWR-0008-16R2

Altered Glycolysis and Mitochondrial Respiration in a Zebrafish Model of Dravet Syndrome

Title: Altered Glycolysis and Mitochondrial Respiration in a Zebrafish Model of Dravet Syndrome

Short Title: Metabolism in scn1Lab mutant Zebrafish

Maneesh G. Kumar[1], Shane Rowley[1], Ruth Fulton[1], Matthew T. Dinday[2], Scott C. Baraban[2], and Manisha Patel[1]

[1]Department of Pharmaceutical Sciences, University of Colorado Anschutz Medical Campus, Aurora, CO 80045

[2]Department of Neurological Surgery, University of California San Francisco, San Francisco, CA 94143

MK, MP, and SB designed research; MK performed research; SR, RF, MD, and SB contributed reagents/analytical tools; MK analyzed data; MK, MP, and SB wrote the paper.

Corresponding author:

Manisha Patel, PhD
University of Colorado
Skaggs School of Pharmacy and Pharmaceutical Sciences
Mail Stop C238 V20-3119
12850 E. Montview Blvd.
Aurora, CO 80045
manisha.patel@ucdenver.edu

Number of Figures: 6

Number of Tables: 1

Number of Multimedia: 0

Number of Words - Abstract: 223

Number of Words - Significance Statement: 68

Number of Words - Introduction: 320

Number of Words - Discussion: 936

Acknowledgements: We would like to thank the zebrafish transgenic core at the University of Colorado (P30NS048154), in particular Dr. Kristin Artinger, Ana-Laura Hernandez, Morgan Singleton and Michelle Tellez.

Authors report no conflict of interest.

This work was supported by the NIH R01NS39587(MP), NIH R01NS079214 (SCB), and (in part) by a sabbatical grant from the Associate Dean of Research Seed Grant Program, Skaggs School of Pharmacy and Pharmaceutical Sciences, University of Colorado.

Abstract

Altered metabolism is an important feature of many epileptic syndromes but has not been reported in Dravet syndrome (DS), a catastrophic childhood epilepsy associated with mutations in a voltage-activated sodium channel, Nav1.1 (SCN1A). To address this, we developed novel methodology to assess real-time changes in bioenergetics in zebrafish larvae between 4 and 6 days post fertilization (dpf). Baseline and 4-aminopyridine (4-AP) stimulated glycolytic flux and mitochondrial respiration were simultaneously assessed using a Seahorse Biosciences extracellular flux analyzer. *Scn1Lab* mutant zebrafish showed a decrease in baseline glycolytic rate and oxygen consumption rate (OCR) compared to controls. A ketogenic diet formulation rescued mutant zebrafish metabolism to control levels. Increasing neuronal excitability with 4-AP resulted in an immediate increase in glycolytic rates in wild-type zebrafish; whereas mitochondrial OCR increased slightly and quickly recovered to baseline values. In contrast, *scn1Lab* mutant zebrafish showed a significantly slower and exaggerated increase of both glycolytic rates and OCR after 4-AP. The underlying mechanism of decreased baseline OCR in *scn1Lab* mutants was not due to altered mitochondrial DNA content or dysfunction of enzymes in the electron transport chain (ETC) or tricarboxylic acid (TCA) cycle. Examination of glucose metabolism using a PCR array identified five glycolytic genes that were down-regulated in *scn1Lab* mutant zebrafish. Our findings in *scn1Lab* mutant zebrafish suggest that glucose and mitochondrial hypometabolism contribute to the pathophysiology of DS.

Significance Statement

These studies demonstrate that metabolism can be studied in zebrafish, and that this novel approach can be used (i) to evaluate chemoconvulsant or genetic zebrafish models of epilepsy or (ii) in metabolism-based drug screening efforts to identify compounds that modulate glycolysis or mitochondrial function. As more models of epilepsy become available, the array of techniques demonstrated here can be used to rapidly characterize metabolic contributions to disease states.

Introduction

Glycolysis and mitochondrial oxidative phosphorylation are key energy producing pathways in the brain. These metabolic pathways may play a role in the control of seizures and epileptogenesis (Rowley et al., 2015). For example, glycolytic rates are acutely increased during ictal activity (Stafstrom et al., 2008) and ictal hypermetabolism in human epileptic foci is followed by interictal hypometabolism, probably resulting from a decreased mitochondrial bioenergetic capacity (Chugani et al., 1994; Lee et al., 2012). Hypometabolism associated with seizures may reflect glucose transport abnormalities or defects in ETC enzymes (Tenney et al., 2014). Seizures are also associated with an imbalance in ATP levels (Grisar, 1984) and represent a common symptom in patients with mitochondrial disease (Wallace et al., 1988; Mecocci et al., 1993; Liang et al., 2012).

Although altered metabolism may be a feature of acquired and/or focal epilepsies, it has not been systematically investigated in any genetic form of epilepsy. Dravet syndrome (DS) is one example of a severe genetic epilepsy most commonly associated with *de novo* mutations in a brain-specific voltage-activated sodium channel (SCN1A). DS children exhibit significant developmental delays, cognitive deficits, behavioral disturbances, and increased risk of sudden unexpected death in epilepsy (SUDEP) (Dravet, 2011). Two types of observations suggest that metabolic dysfunction may be occurring in DS. First, mitochondrial defects in muscle biopsies have been reported in patients. Secondly, some DS children respond positively to treatment with ketogenic diets (KD) (Caraballo, 2011). While numerous mechanisms may underlie the efficacy of KDs (Gano et al., 2014), these observations suggest that energy metabolism is not well studied in DS, or any form of genetic epilepsy. Here we developed novel techniques to show, for the first time, that glycolysis and mitochondrial respiration are abnormal in a zebrafish model of DS and its rescue by a form of a KD. Moreover, altered metabolism in *scn1Lab* mutants was accompanied by downregulation of several glycolytic genes rather than defects in select mitochondrial enzyme activities.

Materials and Methods

Animal Care. *Scn1Lab* mutant zebrafish were obtained from the Baraban lab at the University of California San Francisco (UCSF) and bred in the University of Colorado Anschutz Medical Campus (UCD) zebrafish core facility. When obtained from UCSF, eggs were shipped overnight and immediately placed in a 28.5˚C incubator upon arrival. Zebrafish larvae were maintained in 'embryo medium' consisting of 0.03% Instant Ocean (Aquarium Systems, Inc., Mentor, OH, USA) in deionized water containing 0.2 ppm methylene blue as a fungicide with no additional glucose anapleurotic substrates added. Homozygous mutants (sorted based on pigmentation) and age-matched sibling larvae were used at 4-6 dpf. Pentylenetetrazole (PTZ, Sigma-Aldrich, St. Louis, MO, USA) was dissolved in embryo medium, pH balanced to 7.4, and bath applied. KD water was prepared by sonication of 200 µM palmitate (Sigma-Aldrich, St. Louis, MO, USA) and laurate (Sigma-Aldrich, St. Louis, MO, USA) in embryo media containing 100 µM phosphatidyl choline (Sigma-Aldrich, St. Louis, MO, USA) and bath applied (Taylor et al., 2004).

Metabolic Measurements. Glycolysis and mitochondrial respiration rates were simultaneously measured in live zebrafish in an XF24 or XF24e analyzer (Seahorse Bioscience, North Billerica, MA, USA). One fish was loaded per well of a 24-well islet plate and mesh screen placed to hold the zebrafish in place. 4-AP (Sigma-Aldrich, St. Louis, MO, USA) was prepared in embryo medium at a stock concentration of 40 mM and pH balanced to approximately 7.4. 4-AP was injected by the XF24 analyzer at a final concentration of 4 mM.

Behavioral seizure analysis: Zebrafish were placed individually in 96-well Falcon culture dishes. Each well contained approximately 75 µl embryo media and one 5 days post-fertilization (dpf) WT zebrafish larvae. Swim behavior was monitored in a DanioVision system, as described previously in the literature (Baraban et al., 2013). Recording sessions (2 min) were analyzed off-line and scored for seizure stage (see Baraban et al., 2005) by an investigator blind to the status of the fish.

Mitochondrial Copy Number. Relative mitochondrial copy number was determined by Real-Time PCR (Hunter et al., 2010; Artuso et al., 2012). DNA was extracted from individual fish using the DNeasy Blood and Tissue Kit (Qiagen, Hilden, Germany) following manufacturer supplied instructions. A short section of mitochondrial DNA was amplified using Power SYBR green (Forward: 5'-CAAACACAAGCCTCGCCTGTTTAC-3', Reverse: 5'-CACTGACTTGATGGGGGAGACAGT-3'). This was normalized to the nuclear gene *polg1* (Forward: 5'- GAGAGCGTCTATAAGGAGTAC-3', Reverse: 5'-GAGCTCATCAGAAACAGGACT-3'). Primers were ordered from Integrated DNA Technologies (Coralville, IA, USA). Fish were exposed to 4-AP for 1 hour.

Enzyme Assays. Activity of complexes I-IV was determined from total protein isolates from 25-30 pooled zebrafish embryos at 4-6 dpf. Total protein was isolated by resuspending zebrafish in PBS with 0.01% Triton-X and protease inhibitors followed by probe sonication at 30% intensity for 3 pulses of 5 seconds each. Lysate was centrifuged at 10,000 RPM for 5 minutes to remove insoluble material. Total protein concentration was determined by Bradford assay. Complex activity was determined by UV spectrophotometry (Ma et al., 2011). Complex I was determined by the oxidation of NADH at 340 nm. The assay solution consisted of 25 mM potassium phosphate, 5 mM $MgCl_2$, 2 mM KCN, 2.5 mg/ml BSA, 0.13 mM NADH, 2 ug/mL antimycin A, and 65 µM ubiquinone1 equilibrated to 30˚C. 40 µg of total protein was added and activity measured for 5 minutes. Non-specific activity was determined by addition of 2 µg/mL rotenone prior to protein addition. Complex II was determined by reduction of dichlorophenol indophenols at 600 nm. The assay solution consisted of 25 mM KPO_4, 5 mM $MgCl_2$, 2 mM KCN, 20 mM sodium succinate, 50 µM dichlorophenol indophenol, 2 µg/mL rotenone, and 2 µg/mL antimycin A. After equilibrating to 30˚C, 40 µg of total protein was added along with 65 µM ubiquinone1 to start the reaction. Activity was determined between 3 and 5 minutes. Complex III was determined by the reduction of cytochrome C at 550 nm. The assay solution consisted of 50 mM KPO_4, 1 mM n-dodecyl-B-D-maltoside, 2 mM KCN, and 20 mM NADH at 30˚C. 40 µg of total protein was added along

with 100 µM reduced decylbenzylquinone and 40 µM oxidized cytochrome C to start the reaction. Activity was measured for 3 minutes. Complex IV was determined by oxidation of cytochrome C at 550 nm. The assay solution consisted of 20 mM KPO_4 and 0.45 mM n-dodecyl-B-D-maltoside equilibrated to 30˚C. 40 µg total protein and reduced cytochrome C was added to a final concentration of 15 µM and activity measured for 3 minutes.

Activity of select enzymes of the TCA cycle, aconitase, fumarase, and malate dehydrogenase, was determined from total protein isolates from 30 pooled zebrafish embryos at 5 dpf. Total protein was isolated as above with the exception of probe sonication at 30% intensity for 2 pulses of 1 second each. Aconitase and fumarase activity was determined by UV spectrophotometry by following the dehydration of DL-isocitrate or L-malate, respectively, at 240 nm (Patel et al., 1996). The aconitase assay buffer consisted of 50 mM Tris HCl and 600 µM $MnCl_2$ at a pH of 7.4. DL-Isocitrate substrate was added to a final concentration of 20 mM along with 20 µL of total protein. Activity was measured for 3 minutes. Aconitase activity was inhibited by addition of 0.1 mM potassium ferricyanide. Fumarase assay buffer consisted of 30 mM KH_2PO_4 and 100 µM EDTA at a pH of 7.4. L-malate was added to a final concentration of 5 mM along with 20 µL of total protein. Activity was measured for 3 minutes. Fumarase activity showed stereospecificity for L-malate; D-malate was inactive. Malate dehydrogenase was determined by measuring the decrease in absorbance at 340 nm resulting from oxidation of NADH. The assay buffer consisted of 0.1 M KPO_4, 200 µM oxaloacetic acid, and 250 µM NADH at pH 7.4. 5 µL of total protein was added and activity measured for 5 minutes. All TCA cycle enzyme assays were performed at room temperature.

Gene Expression. Six to eight zebrafish were pooled for each group. RNA was extracted by TRIzol 1 hour after 4-AP treatment. cDNA was synthesized using the RT^2 First Strand Kit (SABiosciences) and hybridized to the Glucose Metabolism PCR array (SABiosciences). Array was analyzed using Applied Biosystem 7500 Real-Time PCR System. Data was analyzed using SABiosciences' online data analysis suite

(http://www.sabiosciences.com/pcrarraydataanalysis.php). Array results were verified using specific Taqman primers (Applied Biosystems). Fish were exposed to 4-AP for 1 hour.

Statistics. Statistical methods were performed with GraphPad Prism v. 6.04 for Windows. Analyses include Holm-Sidak T-Test (for baseline comparisons) and 2-way One Way Analysis of Variance (ANOVA) with Tukey's multiple comparisons test. Behavioral seizure data was analyzed by Shapiro-Wilk normality test followed by Kruskal-Wallis ANOVA on Ranks with Tukey's multiple comparison post-hoc test.

Results

To measure real-time glycolytic and mitochondrial respiration rates live zebrafish (4-6 dpf) were placed in an extracellular flux analyzer (Seahorse Biosciences). The analyzer measures extracellular acidification rate (ECAR) and oxygen consumption rate (OCR) in a transient microchamber over 3 minutes, representing glycolysis and mitochondrial respiration, respectively (Wu, 2009). Baseline glycolysis rates in *scn1Lab* mutant and age-matched WT zebrafish were 7.70 ± 0.18 mpH/min and 13.06 ± 0.61 mpH/min (Figure 1A), respectively, indicating a 41% decrease ($p < 0.0001$)[a] of baseline glycolysis. Similarly, basal OCR was significantly decreased in *scn1Lab* mutant zebrafish (189.3 ± 3.47 pMoles/min) compared to WT controls (296.5 ± 1.929 pMoles/min, $p < 0.0001$[b], Figure 1B). Zebrafish obtained from UCSF or bred at UCD and metabolism measured using the Seahorse XF24 or an updated version, the XF24e, showed similar alterations in metabolism between *scn1Lab* and WT siblings (Figure 6).

Scn1Lab mutant zebrafish have been reported to have seizures very early in life, starting at about 3 dpf (Baraban et al., 2013). To determine the consequences of increased neuronal excitability associated with induced seizure activity, WT zebrafish were stimulated with 4-AP and glycolytic and mitochondrial respiration rates were measured (Figure 1A and 1B). 4-AP, a chemoconvulsant previously shown to induce electrographic seizures in zebrafish (Baraban et al., 2007), increases metabolic demand in cortical cells and synaptosomes (Tibbs et al., 1989; Flynn et al., 2011). Following metabolic challenge

with a single, high dose of 4-AP, WT zebrafish showed increased behavioral seizure activity (Figure 1C and 1D[c-d]) and 360% increase in glycolysis within 8 minutes. *Scn1Lab* mutants, which exhibit spontaneous seizures at a rate of approximately 1 ictal-like event per minute (Baraban et al., 2013), also showed increased glycolytic rate after 4-AP stimulation albeit in a delayed manner, achieving maximal glycolytic rates about 30 minutes after 4-AP addition (Figure 1A). In *scn1Lab* mutant zebrafish, glycolysis was increased 350% from baseline to an average of 27.26 ± 1.12 mpH/min ($p < 0.0001$[e], Figure 1A). Both the immediate and delayed increase of glycolytic rates in WT and *scn1Lab* mutant zebrafish were sustained for the duration of the experiment, 48 minutes. After 24-32 minutes when *scn1Lab* mutant zebrafish had maximal response to 4-AP, the fold change was significantly greater in *scn1Lab* mutant zebrafish than that of WT zebrafish. Behavioral seizure analysis on an independent clutch of WT larvae demonstrated that a single concentration of 4 mM 4-AP induced the severe convulsive seizure behavior (Stage III) at the 8 min time point in 23 out of 48 larvae; circling Stage II behavior was noted in 25 of 48 larvae. After continuous exposure to 4-AP, seizure behavior corresponding to Stage II was observed in the majority of zebrafish larvae (47 out of 48). Representative locomotion plots are shown for WT zebrafish at baseline and following exposure to 4 mM 4-AP (Fig. 1C). Mean velocity measurements, which act as a surrogate marker for Stage III behavior (Baraban et al., 2013) were significantly increased at the 8 min exposure point (Fig. 1D[c]).

WT zebrafish showed a small, non-significant, increase in mitochondrial respiration immediately after 4-AP stimulation which rapidly returned to baseline (Figure 1B). However, *scn1Lab* mutant zebrafish showed a delayed and gradual increase in mitochondrial respiration with maximal increase about 30 minutes after stimulation. Mitochondrial respiration was increased approximately 142% from baseline to 253.1 pMoles/min in *scn1Lab* mutant compared to WT zebrafish.

This data, when plotted as OCR vs. ECAR shows a unique metabolic shift (Figure 2A). At baseline, WT zebrafish are more glycolytic and oxidative than mutant zebrafish, but both processes are in a narrow metabolic field. Increased neuronal excitability shifts the metabolic field towards the glycolytic direction. The mutant zebrafish increase glycolysis and oxidative phosphorylation after 4-AP exposure to approach the metabolic state of WT zebrafish after 4-AP. This suggests that mutant zebrafish retain a similar metabolic capacity as WT zebrafish, or, in other words, there are no defective enzymes in the downstream energetic pathway. To confirm this, we assayed 3 different parameters. To ensure that alterations in mitochondrial OCR were not due to differences in mitochondrial content, relative mitochondrial copy number was determined. Results demonstrate that there is no significant difference between total mitochondrial copy numbers between groups ($p = .2056$[h], Figure 2B). Next, to determine if OCR differences were due to alterations in ETC activity, complexes I-IV were assayed in WT and *scn1Lab* mutant zebrafish. No differences were observed in the activity of any of the complexes ($p = 0.9367$[i], Figure 2C). OCR may also have been decreased in *scn1Lab* mutant zebrafish if the TCA cycle enzymes were inactive, providing fewer electron donors for the ETC. Analysis of aconitase, fumarase, and malate dehydrogenase demonstrated no difference in enzymatic activity in WT and mutant zebrafish ($p = 0.5801$[j], Figure 2D). This suggests that the primary metabolic defect may lie even further upstream, in glycolysis.

We therefore focused on the glycolytic pathway to understand the mechanistic basis of altered metabolism in *scn1Lab* mutant zebrafish. Since the activity of oxidative phosphorylation enzymes were unaltered in *scn1Lab* mutants and previous results suggested that genes related to metabolic processes are differentially expressed in *scn1Lab* mutant zebrafish (Baraban et al., 2007), we examined gene expression changes using an 84 probe glucose metabolism micro-array (Figure 3A and 3B). Of these, 6 genes were changed at least 2-fold (Figure 3C). Five of these 6 were down-regulated in *scn1Lab* mutant zebrafish compared to WT and included *g6pca.1*, *pck1*, *pck2*, *pdk2*, and *phkg1a*. Gene expression was

also analyzed 1 hour after 4-AP treatment. In 4-AP stimulated zebrafish, 4 genes were changed at least 2-fold compared to untreated controls (*gck*, *pck1*, *pdk2*, and *pdk4*). PCR array results were verified using specific Taqman primers which were available for *pck1*, *pck2*, and *pdk2*. PCR results verified fold changes of *pck1* (-2.83 +/- 0.45), *pck2* (-2.36 +/- 0.45), and *pdk2* (-2.23 +/- 0.42) in *scn1Lab* vs. WT zebrafish (Figure 3C, inset). WT zebrafish after 4-AP stimulation were also verified to have a 2.08 +/- 0.48 fold increase in *pdk2* expression; *scn1Lab* mutant zebrafish had a fold-change of 15.16 +/- 4.93 in *pdk2* expression (Figure 3C, inset). These results suggest that baseline decreases in ECAR and OCR in *scn1Lab* mutants likely results from mutation-induced down-regulation of key glycolytic genes leading to an overall decreased flux of substrates through these pathways. Exaggerated responses in ECAR and OCR in *scn1Lab* mutants could be the result of mutation-induced up-regulation of key glycolytic genes (i.e. *pck1* and *pdk2*). Together, alterations in glycolytic gene expression provide a mechanistic basis for ion channel related alterations in metabolism.

Finally, to determine whether metabolic deficits could be rescued, we exposed developing zebrafish larvae to a modified KD (Taylor et al., 2004) for 48 hr. In *scn1Lab* mutant zebrafish, baseline metabolism was raised to levels similar to WT controls for both glycolysis ($p = 0.1043^{k}$) and respiration ($p = 0.9853^{l}$) (Figure 4A). 4-AP treatment produced a similar magnitude of increase in ECAR in both vehicle and KD-exposed WT controls ($p = 0.4744^{m}$), however, the response to 4-AP was suppressed in the KD-exposed *scn1Lab* mutant zebrafish to the same rates as WT zebrafish ($p = 0.1294^{n}$) (Figure 4B).

Discussion

Here we demonstrate significant decreases in metabolism in a zebrafish model of SCN1A-related epilepsy. These mutants exhibit hyperactivity, including convulsive behavior, spontaneous electrographic seizures, shortened lifespan and a pharmacological profile similar to the human condition (Baraban et al., 2013; Dinday and Baraban, 2015). We now demonstrate, using novel methodology, that these *scn1Lab* mutant zebrafish, representing one example of a genetic epilepsy, exhibit decreased

glycolytic and mitochondrial respiration rates. Although mitochondrial respiration has been measured in early embryogenesis up to 48 hours post fertilization (Stackley et al., 2011) and cell-based (Gimenez-Cassina et al., 2012) or rodent-based (Rowley et al., 2015) systems, this is the first time metabolism has been measured in live zebrafish larvae and could be useful in identifying metabolic dysfunction in the growing armamentarium of zebrafish mutants.

Hypometabolism in DS has not been extensively reported in the literature. However, in a single study evaluating the metabolic status of patients with DS, Craig *et. al* (2012) showed co-morbid electron transport defects in two patients. One had impaired complex III activity, and the other complex IV, in muscle biopsy from two DS patients. The etiology of the co-morbidity is not entirely obvious but the authors suggest an SCN1A mutation is not the only cause. Our results support these suppositions. The *scn1Lab* mutant zebrafish did not show any defects in ETC complexes I-IV, suggesting respiratory chain defects may not be inherent to DS.

The mechanism by which loss of sodium channel function results in the constellation of symptoms observed in DS is incompletely understood. Our results suggest a general decrease in expression of glycolysis related genes resulting in decreased glycolytic substrates driving mitochondrial respiration. It is possible seizures, which are spontaneously occurring in these mutants, induce oxidative stress resulting in posttranslational oxidative modification and decreased activities of complex I (Ryan et al., 2012). Metabolic dysfunction, in particular mitochondrial dysfunction, has been known to have epilepsy as a dominant or collateral feature of the phenotype (Finsterer and Zarrouk Mahjoub, 2012). In addition, mitochondrial complex I deficiency has been observed in human and experimental temporal lobe epilepsy (Kunz et al., 2000). Whether the presence of seizures alone explains the metabolic deficits is unclear and needs further exploration.

Interestingly and consistent with a metabolic defect, KDs have shown efficacy in controlling seizures in some DS patients (Caraballo, 2011) and the *scn1Lab* mutant zebrafish used here (Baraban et

al., 2013). We now show that a KD also improves the metabolic state of *scn1Lab* mutant zebrafish to WT levels. One potential mechanism of action is that the KD alters expression of glucose-related metabolism genes in *scn1Lab* mutant zebrafish to WT levels. However, this seems unlikely as alteration of the genes reported here, and others, by KD has not been reported in the literature. Murata et al. (2013) fed WT and *Fgf21* (fibroblast growth factor) knockout mice KD and showed no difference in *pck* expression, or glucose-6-phosphatase and PPARɣ coactivator-1α, compared to normal diet. Jornayvaz et al. (2010) showed similar results in KD fed mice for *pck*, glucose-6-phosphatase, and pyruvate carboxylase compared to control diet. However, a more likely mechanism is that a KD alters the fuels available for glycolysis and oxidative phosphorylation to use. Impairment of mitochondrial bioenergetics capacity can critically affect apoptosis, neuronal excitability, and seizure susceptibility (Gano et al., 2014). Ketone bodies can decrease the spontaneous firing of GABAergic neurons, dependent on K_{ATP} channels (Ma et al., 2007) and given the deficits in interneuron function thought to be associated with SCN1A mutation this could be a direct site of action.

4-AP is a potassium channel blocker that is commonly used to elicit seizures in animal models, including larval zebrafish (Baraban et al., 2007). Here, we demonstrate that WT zebrafish respond to 4-AP by immediately increasing glycolysis but not mitochondrial respiration corresponding with severe behavioral seizures. The metabolic alteration is reminiscent of ictal hypermetabolism (Stafstrom et al., 2008) and it is interesting to note that *scn1Lab* mutants have delayed increases in glycolysis and mitochondrial respiration after a 4-AP challenge. We also report a significant downregulation of phosphoenolpyruvate carboxykinases (*pck1* and *pck2*) and pyruvate dehydrogenase kinase (*pdk2*) in *scn1Lab* mutant, genes important in gluconeogenesis, glycogenolysis, and regulation of pyruvate dehydrogenase. Specifically, *pck* is responsible for converting oxaloacetate in to phosphoenolpyruvate, a glycolysis intermediary and its loss would result in less intermediates and less glycolytic flux. *Pdk2* is a gene responsible for inhibition of pyruvate dehydrogenase which converts pyruvate to acetyl CoA.

Decreased *pdk2* would result in increased pyruvate dehydrogenase activity and less pyruvate and lactate. This could explain the lower ECAR observed here (Sun et al., 2011). It may appear that increased pyruvate dehydrogenase would result in increased respiration in *scn1Lab* mutant zebrafish. However, because there are fewer intermediates, and less flux through glycolysis, it is reasonable that the overall respiration rate is reduced in *scn1Lab* mutant zebrafish. In WT zebrafish, the increase in *pdk2* would increase inhibition of pyruvate dehydrogenase and subsequently lead to increases in glycolytic metabolites pyruvate and lactate, suggesting a mechanism for increased glycolysis.

Overall, our results suggest a metabolic impairment concomitant with a sodium channel mutation in DS, likely due to glycolysis gene expression changes and reversible by the KD (Figure 5). We demonstrate this with a novel technique to assess ECAR and OCR in live zebrafish and propose that the metabolic impairment in *scn1Lab* mutant zebrafish may be due to changes in gene expression related to glucose metabolism (Figure 3B). This approach was applied here to one genetic model of epilepsy, but opens new avenues for studying metabolism in any zebrafish model or as means to screen compound libraries for new drugs that would improve metabolic function.

References

Artuso L, Romano A, Verri T, Domenichini A, Argenton F, Santorelli FM, Petruzzella V (2012) Mitochondrial DNA metabolism in early development of zebrafish (Danio rerio). Biochimica et biophysica acta 1817:1002-1011.

Baraban SC, Taylor MR, Castro PA, Baier H (2005) Pentylenetetrazole induced changes in zebrafish behavior, neural activity and c-Fos expression. Neuroscience 131:659-768.

Baraban SC, Dinday MT, Hortopan GA (2013) Drug screening in Scn1a zebrafish mutant identifies clemizole as a potential Dravet syndrome treatment. Nature communications 4:2410.

Baraban SC, Dinday MT, Castro PA, Chege S, Guyenet S, Taylor MR (2007) A large-scale mutagenesis screen to identify seizure-resistant zebrafish. Epilepsia 48:1151-1157.

Caraballo RH (2011) Nonpharmacologic treatments of Dravet syndrome: focus on the ketogenic diet. Epilepsia 52 Suppl 2:79-82.

Chugani HT, Rintahaka PJ, Shewmon DA (1994) Ictal patterns of cerebral glucose utilization in children with epilepsy. Epilepsia 35:813-822.

Craig AK, de Menezes MS, Saneto RP (2012) Dravet syndrome: patients with co-morbid SCN1A gene mutations and mitochondrial electron transport chain defects. Seizure : the journal of the British Epilepsy Association 21:17-20.

Dinday MT, Baraban SC (2015) Large-Scale Phenotype-Based Antiepileptic Drug Screening in a Zebrafish Model of Dravet Syndrome(1,2,3). eNeuro 2.

Dravet C (2011) The core Dravet syndrome phenotype. Epilepsia 52 Suppl 2:3-9.

Finsterer J, Zarrouk Mahjoub S (2012) Epilepsy in mitochondrial disorders. Seizure : the journal of the British Epilepsy Association 21:316-321.

Flynn JM, Choi SW, Day NU, Gerencser AA, Hubbard A, Melov S (2011) Impaired spare respiratory capacity in cortical synaptosomes from Sod2 null mice. Free radical biology & medicine 50:866-873.

Gano LB, Patel M, Rho JM (2014) Ketogenic diets, mitochondria, and neurological diseases. Journal of lipid research 55:2211-2228.

Gimenez-Cassina A, Martinez-Francois JR, Fisher JK, Szlyk B, Polak K, Wiwczar J, Tanner GR, Lutas A, Yellen G, Danial NN (2012) BAD-dependent regulation of fuel metabolism and K(ATP) channel activity confers resistance to epileptic seizures. Neuron 74:719-730.

Grisar T (1984) Glial and neuronal Na+-K+ pump in epilepsy. Annals of neurology 16 Suppl:S128-134.

Hunter SE, Jung D, Di Giulio RT, Meyer JN (2010) The QPCR assay for analysis of mitochondrial DNA damage, repair, and relative copy number. Methods 51:444-451.

Jornayvaz FR, Jurczak MJ, Lee HY, Birkenfeld AL, Frederick DW, Zhang D, Zhang XM, Samuel VT, Shulman GI (2010) A high-fat, ketogenic diet causes hepatic insulin resistance in mice, despite increasing energy expenditure and preventing weight gain. Am J Physiol Endocrinol Metab 299:E808-815.

Kunz WS, Kudin AP, Vielhaber S, Blumcke I, Zuschratter W, Schramm J, Beck H, Elger CE (2000) Mitochondrial complex I deficiency in the epileptic focus of patients with temporal lobe epilepsy. Annals of neurology 48:766-773.

Lee EM, Park GY, Im KC, Kim ST, Woo CW, Chung JH, Kim KS, Kim JS, Shon YM, Kim YI, Kang JK (2012) Changes in glucose metabolism and metabolites during the epileptogenic process in the lithium-pilocarpine model of epilepsy. Epilepsia 53:860-869.

Liang LP, Waldbaum S, Rowley S, Huang TT, Day BJ, Patel M (2012) Mitochondrial oxidative stress and epilepsy in SOD2 deficient mice: attenuation by a lipophilic metalloporphyrin. Neurobiology of disease 45:1068-1076.

Ma W, Berg J, Yellen G (2007) Ketogenic diet metabolites reduce firing in central neurons by opening K(ATP) channels. The Journal of neuroscience : the official journal of the Society for Neuroscience 27:3618-3625.

Ma YY, Zhang XL, Wu TF, Liu YP, Wang Q, Zhang Y, Song JQ, Wang YJ, Yang YL (2011) Analysis of the mitochondrial complex I-V enzyme activities of peripheral leukocytes in oxidative phosphorylation disorders. Journal of child neurology 26:974-979.

Mecocci P, MacGarvey U, Kaufman AE, Koontz D, Shoffner JM, Wallace DC, Beal MF (1993) Oxidative damage to mitochondrial DNA shows marked age-dependent increases in human brain. Annals of neurology 34:609-616.

Murata Y, Nishio K, Mochiyama T, Konishi M, Shimada M, Ohta H, Itoh N (2013) Fgf21 impairs adipocyte insulin sensitivity in mice fed a low-carbohydrate, high-fat ketogenic diet. PloS one 8:e69330.

Patel M, Day BJ, Crapo JD, Fridovich I, McNamara JO (1996) Requirement for superoxide in excitotoxic cell death. Neuron 16:345-355.

Rowley S, Liang LP, Fulton R, Shimizu T, Day B, Patel M (2015) Mitochondrial respiration deficits driven by reactive oxygen species in experimental temporal lobe epilepsy. Neurobiology of disease 75:151-158.

Ryan K, Backos DS, Reigan P, Patel M (2012) Post-translational oxidative modification and inactivation of mitochondrial complex I in epileptogenesis. The Journal of neuroscience : the official journal of the Society for Neuroscience 32:11250-11258.

Stackley KD, Beeson CC, Rahn JJ, Chan SS (2011) Bioenergetic profiling of zebrafish embryonic development. PloS one 6:e25652.

Stafstrom CE, Roopra A, Sutula TP (2008) Seizure suppression via glycolysis inhibition with 2-deoxy-D-glucose (2DG). Epilepsia 49 Suppl 8:97-100.

Sun W, Chang SS, Fu Y, Liu Y, Califano JA (2011) Chronic CSE treatment induces the growth of normal oral keratinocytes via PDK2 upregulation, increased glycolysis and HIF1alpha stabilization. PloS one 6:e16207.

Taylor MR, Hurley JB, Van Epps HA, Brockerhoff SE (2004) A zebrafish model for pyruvate dehydrogenase deficiency: rescue of neurological dysfunction and embryonic lethality using a ketogenic diet. Proceedings of the National Academy of Sciences of the United States of America 101:4584-4589.

Tenney JR, Rozhkov L, Horn P, Miles L, Miles MV (2014) Cerebral glucose hypometabolism is associated with mitochondrial dysfunction in patients with intractable epilepsy and cortical dysplasia. Epilepsia 55:1415-1422.

Tibbs GR, Barrie AP, Van Mieghem FJ, McMahon HT, Nicholls DG (1989) Repetitive action potentials in isolated nerve terminals in the presence of 4-aminopyridine: effects on cytosolic free Ca2+ and glutamate release. Journal of neurochemistry 53:1693-1699.

Tiedeken JA, Ramsdell JS (2007) Embryonic exposure to domoic Acid increases the susceptibility of zebrafish larvae to the chemical convulsant pentylenetetrazole. Environ Health Perspect 115:1547-1552.

Wallace DC, Zheng XX, Lott MT, Shoffner JM, Hodge JA, Kelley RI, Epstein CM, Hopkins LC (1988) Familial mitochondrial encephalomyopathy (MERRF): genetic, pathophysiological, and biochemical characterization of a mitochondrial DNA disease. Cell 55:601-610.

Wu M (2009) Real-Time Measurement of Mitochondrial Respiration and Glycolysis Rates of Cancer Cells in a Microplate. In, pp 295-300.

Legends:

Figure 1: Glycolytic and mitochondrial respiration rates in WT and *scn1Lab* mutant zebrafish at baseline and after 4-AP stimulation. **A and B.** *Scn1Lab* mutant zebrafish have lower baseline glycolytic and mitochondrial respiration rates than WT zebrafish. 4-AP immediately increases glycolytic and mitochondrial respiration rates in WT zebrafish. *Scn1Lab* mutant zebrafish have a delayed response to 4-AP of about 30 minutes. Statistical analysis shows changes relative to time-matched untreated controls. N = 14 (WT), 16 (*scn1Lab*), 16 (WT+4-AP), 14 (*scn1Lab*+4-AP) individual animals. A. WT vs. *scn1Lab*, p < 0.0001[a]. WT vs WT+4-AP, p = 2.38e-30 (8 min)[o], p = 8.41e-30 (16 min)[p], p = 3.50e-26 (24 min)[q], p = 3.99e-24 (32 min)[r], p = 2.92e-25 (40 min)[s], p = 1.70e-21 (48 min)[t]. *scn1Lab* vs *scn1Lab*+4-AP, p = 3.28e-6 (8 min)[u], p = 1.65e-11 (16 min)[v], p = 1.86e-13 (24 min)[w], p = 3.08e-17 (32 min)[x], p = 2.34e-14 (40 min)[y], p = 3.52e-15 (48 min)[z]. B. WT vs. *scn1Lab* p < 0.0001[aa]. *scn1Lab* vs. *scn1Lab*+4-AP, p = 0.00071 (32 min)[bb], p = 2.20e-5 (40 min)[cc], p = 7.24e-5 (48 min)[dd]. **C and D**. Locomotion plots for behavioral seizure activity in

WT zebrafish exposed to 4 mM 4-AP. Bar plot showing the mean ± S.E.M. for WT fish at baseline, 8 min after exposure to 4-AP and 48 min after exposure to 4-AP. N = 48 WT fish. Kruskal-Wallis one-way analysis of variance on ranks with a post hoc Tukey test, $p < 0.05$ (8 min v. baseline).

Figure 2: Respiratory chain complex activity in WT and *scn1Lab* mutant zebrafish. A. ECAR and OCR from Figure 1 are replotted to demonstrate the metabolic field and the increases in metabolic field after treatment with 4-AP. *Scn1Lab* mutant zebrafish increase metabolism to approach the metabolic state of WT zebrafish after 4-AP, suggesting mutant zebrafish retain a similar metabolic capacity as WT zebrafish. **B.** Relative mitochondrial copy number was determined by total mitochondrial DNA. No significant differences were found (n = 3 individual animals per group, one-way ANOVA $p = 0.2056$[gg]). **C.** There is no difference in activity in complexes I-IV in WT and *scn1Lab* mutant zebrafish. Bars represent the mean +/- SEM relative to WT activity, n = 3 groups with 25-30 fish pooled per group. Two-way ANOVA, interaction $p = 0.9367$[hh]. **D.** There are no differences in activity in selected TCA cycle enzymes in WT and *scn1Lab* mutant zebrafish. Bars represent the mean +/- SEM relative to WT activity, n = 4 groups with 30 fish per group. Two-way ANOVA, interaction $p = 0.5801$[ii].

Figure 3: Glucose Metabolism related gene expression in WT and *scn1Lab* mutant zebrafish at baseline and after 4-AP stimulation. A. Heatmap demonstrating relative expression of all genes analyzed from array. **B.** Schematic depicting the pathways in which up or down-regulated genes are involved. Red color indicates downregulated genes in scn1Lab mutant zebrafish vs. WT at baseline. **C.** Graph showing the 7 genes with 2-fold or greater changes relative to respective controls. n=6 pooled embryos per group analyzed once. Inset shows PCR verification of genes for which specific primers were available, *pck2, pck4,* and *pdk2*. N = 3 groups of pooled embryos (6 per group) analyzed in triplicate.

Figure 4: Ketogenic diet restores metabolism of *scn1Lab* mutant zebrafish to WT levels. A. Metabolic profile of WT zebrafish is shifted slightly to be more glycolytic after KD treatment. Mutant zebrafish increase both glycolysis and mitochondrial respiration to WT levels. **B.** KD treatment reduces mutant zebrafish response to 4-AP to similar to WT levels. N = 4 (WT), 4 (*scn1Lab*), 5 (WT+KD), 5 (*scn1Lab*+KD), p = .017[jj].

Figure 5: Summary diagram depicting proposed mechanism. A. Mechanism demonstrating changes in glycolysis and mitochondrial respiration in *scn1a* mutant zebrafish at baseline (in black) and proposed action of KD (in red).

Figure 6: Metabolic differences in WT and *scn1lab* mutant zebrafish are reproducible when grown in a separate facility as well as with different instrumentation. All zebrafish in this figure were bred and grown at [Author's Institution]. Using the same instrumentation as Figures 1 and 4 (XF24) the baseline differences are recapitulated in zebrafish grown at [Author's Institution]. The newer model of extracellular flux analysis (XF24e) is more sensitive and thus has higher baseline values for both glycolysis and mitochondrial respiration. **A and B.** Absolute baseline differences in glycolysis and respiration are recapitulated in both the XF24 and newer XF24e. A. XF24, p < .000[kk]. XF24e, p < .00[ll]. B. XF24, p = .00[mm]. XF24e, p < .00[nn]. **C and D.** Although the XF24e is more sensitive, the relative differences in glycolysis and respiration are similar in both the XF24 and XF24e. C. XF24, p < .00[oo]. XF24e, p < .00[pp]. D. XF24, p = .0002[qq]. XF24e, p < .0001[rr].

Table 1: Stats Table

	Data Structure	Type of Test	Confidence Interval
a	Normal distribution	T-test	-6.78 to -3.94
b	Normal distribution	T-test	-116.0 to -98.31
c	Non-normal distribution (Shapiro-Wilk test p<0.05)	One-way ANOVA Kruskal-Wallis on ranks with a post hoc Tukey test	P<0.01 ANOVA 8 min vs Baseline : P<0.05
d	Non-normal distribution (Shapiro-Wilk test p<0.05)	One-way ANOVA	Baseline vs 48 min: P>0.05
e	Normal distribution	Unpaired T-test	-23.76 to -15.36
f	Normal distribution	T-Test with Holm-Sidak for multiple comparisons	-245.2 to -110.5
g	Normal distribution	T-Test with Holm-Sidak for multiple comparisons	-64.78 to -20.95
h	Normal distribution	One-way ANOVA	WT vs. WT+4-AP -0.9128 to 0.1422 WT vs. *scn1Lab* -0.5763 to 0.4787 WT vs. *scn1Lab*+4-AP -0.5664 to 0.4886
i	Normal distribution	Two-way ANOVA	Complex I -148.8 to 112.6 Complex II -138.4 to 123.1 Complex III -177.9 to 83.56 Complex IV -146.6 to 114.9
j	Normal distribution	Two-way ANOVA	Aconitase -15.04 to 45.86 Fumarase -32.52 to 28.38 Mal. Dehyd. -21.06 to 33.41
k	Normal distribution	T-Test	-0.3722 to 3.172
l	Normal distribution	T-Test	65.33 to 64.27
m	Normal distribution	T-Test	-236.8 to 132.0
n	Normal distribution	T-Test	-1.676 to 0.3118
o	Normal distribution	T-Test with Holm-Sidak for multiple comparisons	-33.97 to -22.24
p	Normal distribution	T-Test with Holm-Sidak for multiple comparisons	-33.59 to -21.85
q	Normal distribution	T-Test with Holm-Sidak for multiple comparisons	-31.04 to -19.30
r	Normal distribution	T-Test with Holm-Sidak for multiple comparisons	-29.59 to -17.86
s	Normal distribution	T-Test with Holm-Sidak for multiple comparisons	-30.39 to -18.66
t	Normal distribution	T-Test with Holm-Sidak for multiple comparisons	-27.73 to -16.00

u	Normal distribution	T-Test with Holm-Sidak for multiple comparisons	-18.01 to -6.278
v	Normal distribution	T-Test with Holm-Sidak for multiple comparisons	-24.10 to -12.37
w	Normal distribution	T-Test with Holm-Sidak for multiple comparisons	-26.07 to -14.33
x	Normal distribution	T-Test with Holm-Sidak for multiple comparisons	-29.68 to -17.95
y	Normal distribution	T-Test with Holm-Sidak for multiple comparisons	-26.95 to -15.21
z	Normal distribution	T-Test with Holm-Sidak for multiple comparisons	-27.74 to -16.01
aa	Normal distribution	T-Test	-116.0 to -98.31
bb	Normal distribution	T-Test with Holm-Sidak for multiple comparisons	-112.2 to -6.900
cc	Normal distribution	T-Test with Holm-Sidak for multiple comparisons	-128.0 to -22.77
dd	Normal distribution	T-Test with Holm-Sidak for multiple comparisons	-122.9 to -17.64
ee	Normal distribution	One-way ANOVA	Control vs. 10 μM -3.649 to 7.982 Control vs. 50 μM -6.585 to 5.046 Control vs. 100 μM -4.812 to 6.819 Control vs. 1 mM -6.324 to 5.307 Control vs. 4 mM -7.943 to 2.825
ff	Normal distribution	One-way ANOVA	Control vs. 10 μM -67.77 to 93.79 Control vs. 50 μM -62.06 to 99.49 Control vs. 100 μM -39.08 to 122.5 Control vs. 1 mM -19.22 to 142.3 Control vs. 4 mM -19.85 to 129.7
gg	Normal distribution	One-way ANOVA	WT vs. WT+4-AP -0.9128 to 0.1422 WT vs. *scn1Lab* -0.5763 to 0.4787 WT vs. *scn1Lab*+4-AP -0.5664 to 0.4886
hh	Normal distribution	Two-way ANOVA	Complex I -148.8 to 112.6 Complex II -138.4 to 123.1 Complex III -177.9 to 83.56 Complex IV -146.6 to 114.9
ii	Normal distribution	Two-way ANOVA	Aconitase -15.04 to 45.86 Fumarase -32.52 to 28.38 Mal. Dehyd. -21.06 to 33.41
jj	Normal distribution	T-Test	1.783 to 8.531
kk	Normal distribution	T-Test	-4.128 to -2.727
ll	Normal distribution	T-Test	-36.51 to -22.87
mm	Normal distribution	T-Test	-98.59 to -32.08
nn	Normal distribution	T-Test	-104.4 to -49.14
oo	Normal distribution	T-Test	-46.07 to -30.43
pp	Normal distribution	T-Test	-52.57 to -32.94

qq	Normal distribution	T-Test	-35.93 to -11.69
rr	Normal distribution	T-Test	-32.95 to -15.50

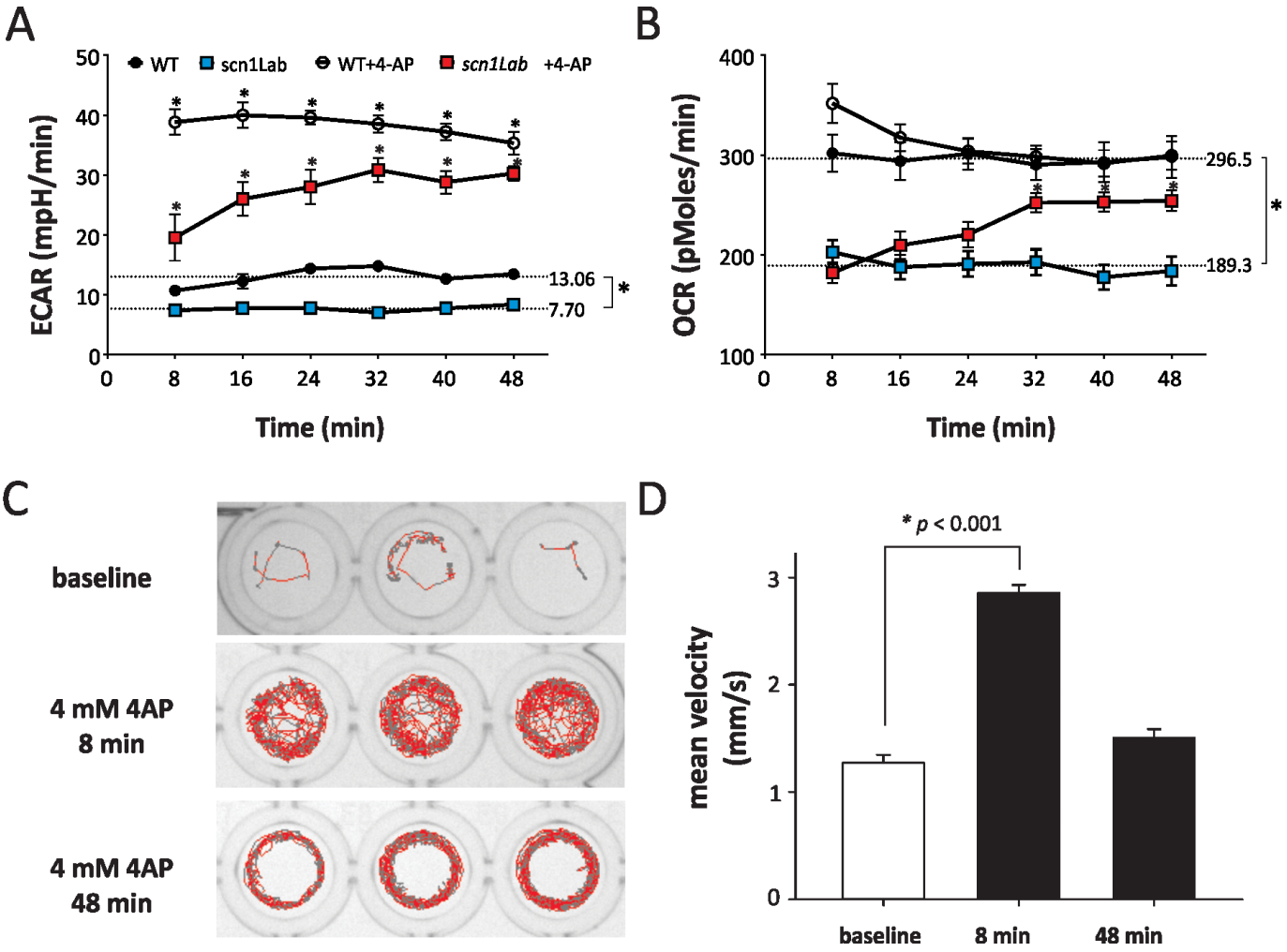

A.

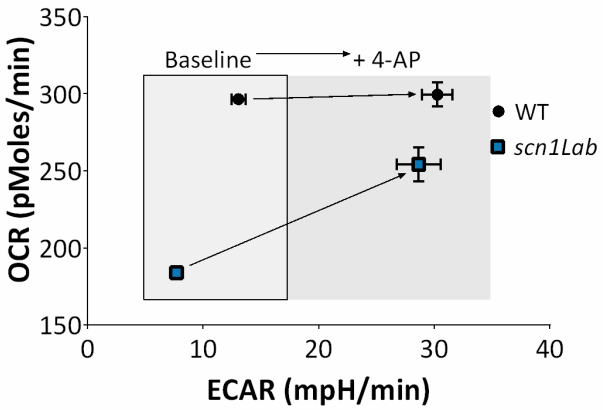

B.

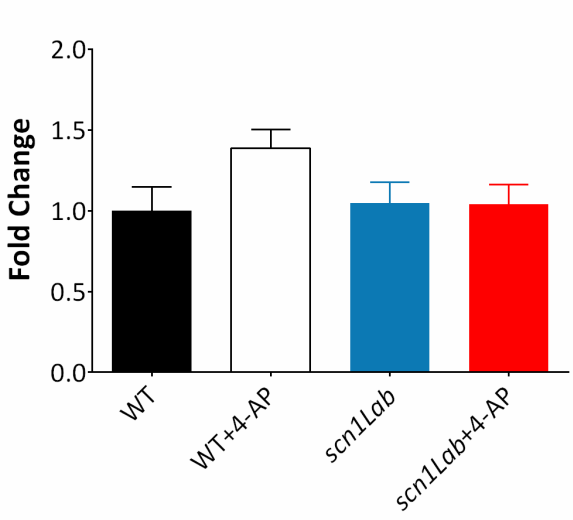

C.

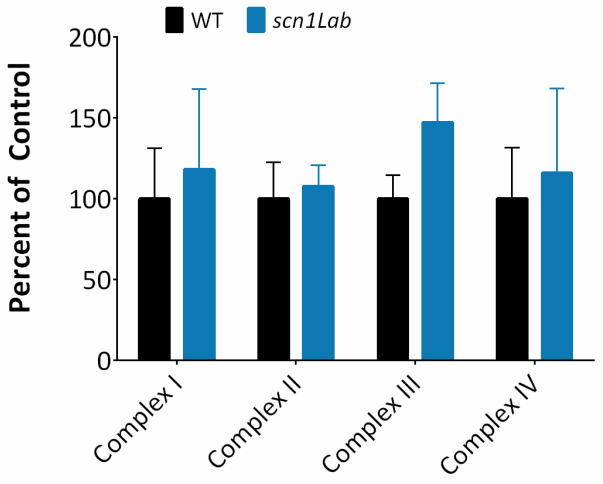

D.

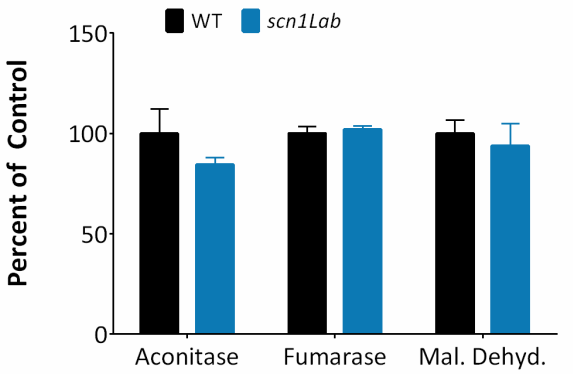

A.

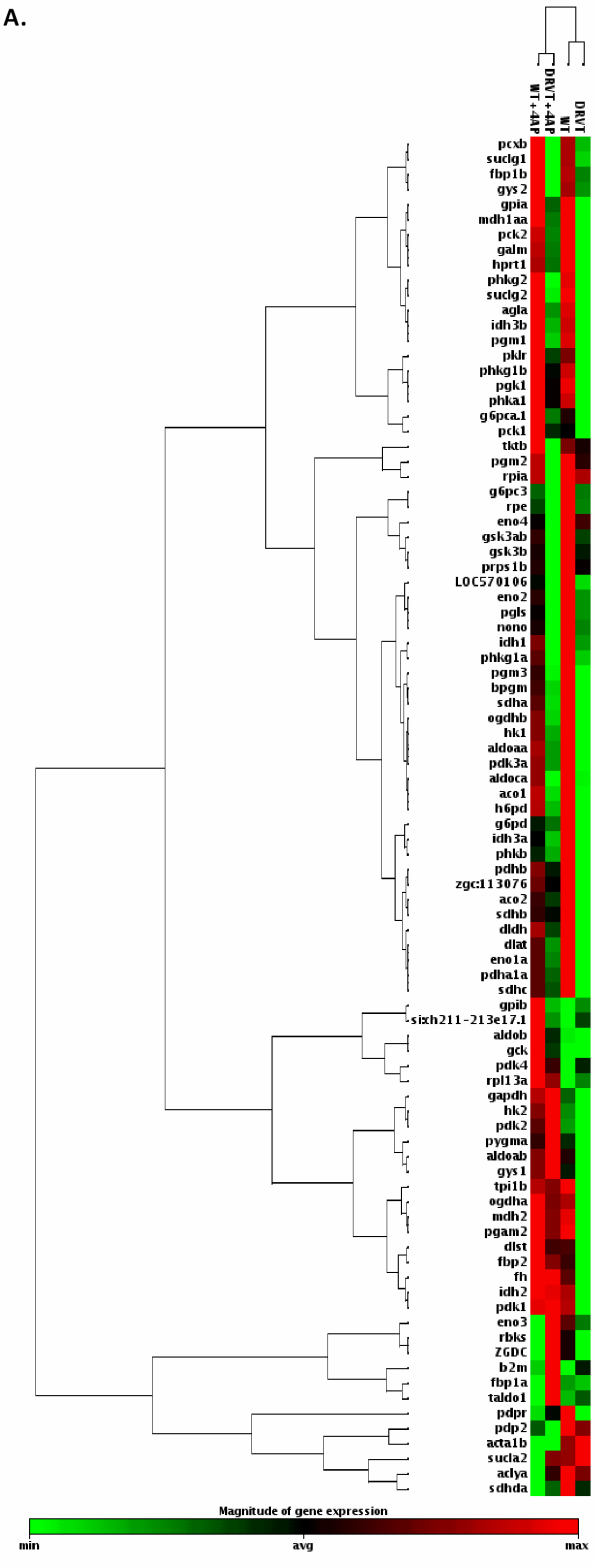

B.

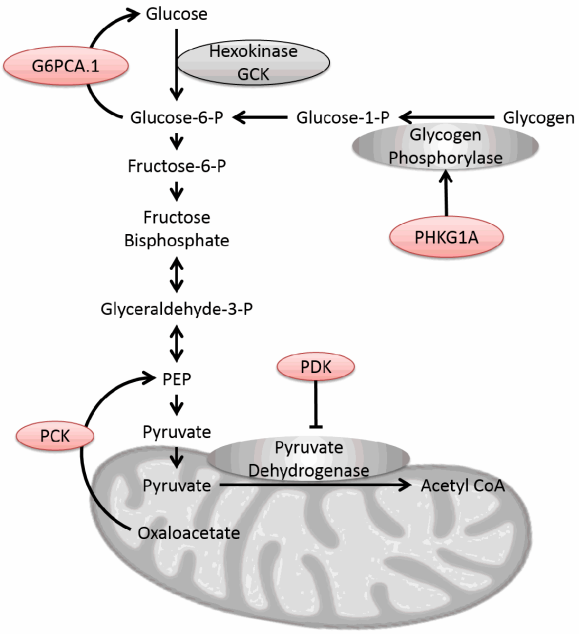

C.

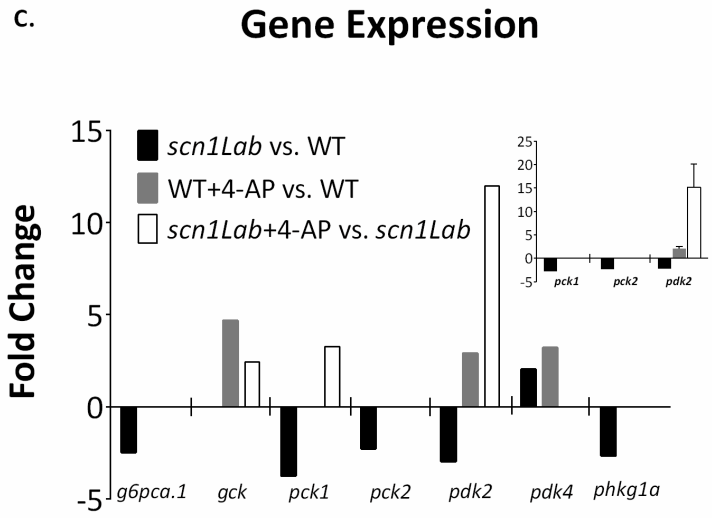

A.

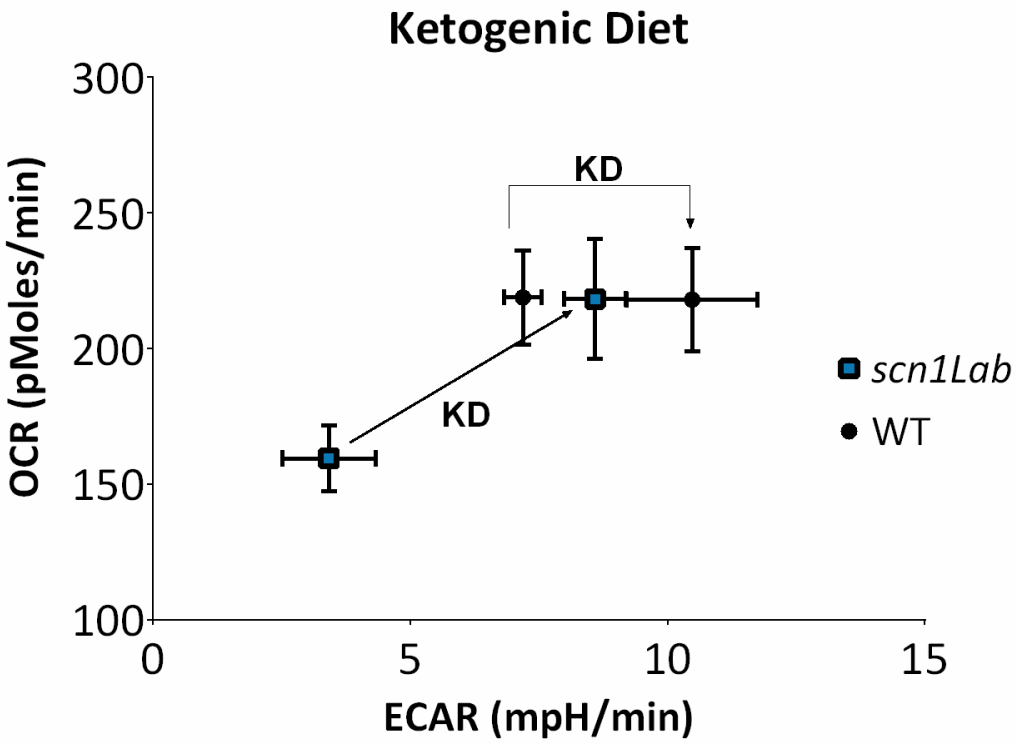

B.